Structure-Dependent Strain Effects

Downloaded from: https://research.chalmers.se, 2026-04-04 23:49 UTC

Citation for the original published paper (version of record):
Dietze, E., Grönbeck, H. (2020). Structure-Dependent Strain Effects. ChemPhysChem, 21(21): 2407-2410. http://dx.doi.org/10.1002/cphc.202000694

N.B. When citing this work, cite the original published paper.

research.chalmers.se offers the possibility of retrieving research publications produced at Chalmers University of Technology. It covers all kind of research output: articles, dissertations, conference papers, reports etc. since 2004. research.chalmers.se is administrated and maintained by Chalmers Library

(article starts on next page)

Structure-Dependent Strain Effects

Elisabeth M. Dietze*[a] and Henrik Grönbeck*[a]

Density functional theory calculations of atomic and molecular adsorption on (111) and (100) metal surfaces reveal marked surface and structure dependent effects of strain. Adsorption in three-fold hollow sites is found to be destabilized by compressive strain whereas the reversed trend is commonly valid for adsorption in four-fold sites. The effects, which are qualitatively explained using a simple two-orbital model, provide insights on how to modify chemical properties by strain design.

Heterogenous catalysts[1,2] are commonly realized as nanoparticles dispersed on oxide supports. The nanoparticles expose a variety of different surface sites, such as terrace, edge, and corner sites, with distinct adsorption and reaction properties.[3–5] The reactivity is, moreover, affected by the fact that the surface atoms of nanoparticles are strained. One reason for the strain, is the finite size and the arrangement to shapes that minimize the surface energy.[6,7] Nanoparticles may additionally be strained by the lattice mismatch to the support.[8] This type of external strain offers a possibility to modify and, ultimately, tailor reaction properties.[9–11]

The dependence of adsorption energies on transition metal and type of site has over the past decades been rationalized by different types of scaling relations.[12,13] The *d*-band model is one important example, which relates the adsorption energy with the position of the *d*-band center with respect to the Fermi energy.[12] The model, which commonly have been applied to (111) terraces, predict that the adsorption energy increases (decreases) when the *d*-band center is moved closer to (further away from) the Fermi energy. An alternative scaling relation that instead employ structural properties and enable comparisons between different adsorption sites, is the generalized coordination number.[13,14] Robust scaling relations are important to rationalize trends in adsorption properties and to obtain reactivity properties using Brønsted-Evans-Polanyi relations.[15]

The effect of strain on adsorption properties has in the past been rationalized within the *d*-band model[11,16] focusing on adsorption on (111) surfaces. To maintain the *d*-band filling, the *d*-band center ε_d shifts closer to the Fermi energy for tensile strain, whereas it shifts away from the Fermi energy for compressive strain. From the (111) data, it was concluded that tensile (compressive) strain is increasing (decreasing) the adsorption energy. These trends have, for example, been confirmed experimentally by studies of CO adsorption on strained Pt surfaces.[17] Effects of strain have also been incorporated in an extension of the generalized coordination number, which has been applied to adsorption on strained Pt and Au sites.[18]

Scaling relations have mainly been developed in connection to atomic and molecular adsorption on close packed surfaces, such as the (111) surface for fcc-metals. However, nanoparticles expose a variety of surfaces including (100) facets and the kinetic coupling between the different facets could be important for catalytic properties.[19] Here we study the effect of strain on different surfaces and obtain previously overlooked phenomena. We find that the response of strain to the adsorption energy depends on adsorbate, metal and type of site.

Density functional theory calculations are used to investigate the effect of symmetric strain in (111) and (100) surfaces of Pd, Pt and Rh for atomic adsorbates (H, B, C, N, O and F) and molecular fragments (OH, CH and CO) at the three-fold hollow fcc site on the (111) surface and the four-fold hollow site on the (100) surface. The calculations are done with the PBE[20] functional as implemented in VASP 5.4.4.[21–23] The surfaces are described by four-layer slabs with either 2×2 or 3×3 surface cells. Adsorption is studied with coverages of 1/4 or 1/9, respectively. The metals and adsorbates are chosen based on their importance in a range of industrial processes, such as fuel synthesis and emission control. H, C, O, OH, CO and CH are, for example, surface species during methane oxidation and CO_2 hydrogenation.[24–26]

Figure 1 shows the relative adsorption energies with respect to the unstrained surfaces for the three-fold hollow fcc site on (111) and four-fold hollow site on (100) of Rh, Pd and Pt for both compressive and tensile strain. The effect of strain for the (111) surfaces is in agreement with previous studies[11,27] and the trends are similar across all investigated atoms and molecular fragments; Compressive (tensile) strain results in lower (higher) adsorption energy. For atomic adsorbates, the change in adsorbate energy with strain is largest for Pt, followed by the other metals. The situation is less clear for the molecular adsorbates, where no general trend is observed between the metals.

The influence of strain for adsorption in the four-fold hollow site on the (100) surface is varying strongly with the adsorbed species and the considered metal. For hydrogen adsorption on

[a] Dr. E. M. Dietze, Prof. Dr. H. Grönbeck
Department of Physics and Competence Centre for Catalysis
Chalmers University of Technology
41296 Göteborg (Sweden)
E-mail: dietze@chalmers.se
ghj@chalmers.se

Supporting information for this article is available on the WWW under https://doi.org/10.1002/cphc.202000694

© 2020 The Authors. Published by Wiley-VCH GmbH. This is an open access article under the terms of the Creative Commons Attribution Non-Commercial NoDerivs License, which permits use and distribution in any medium, provided the original work is properly cited, the use is non-commercial and no modifications or adaptations are made.

© 2020 The Authors. Published by Wiley-VCH GmbH

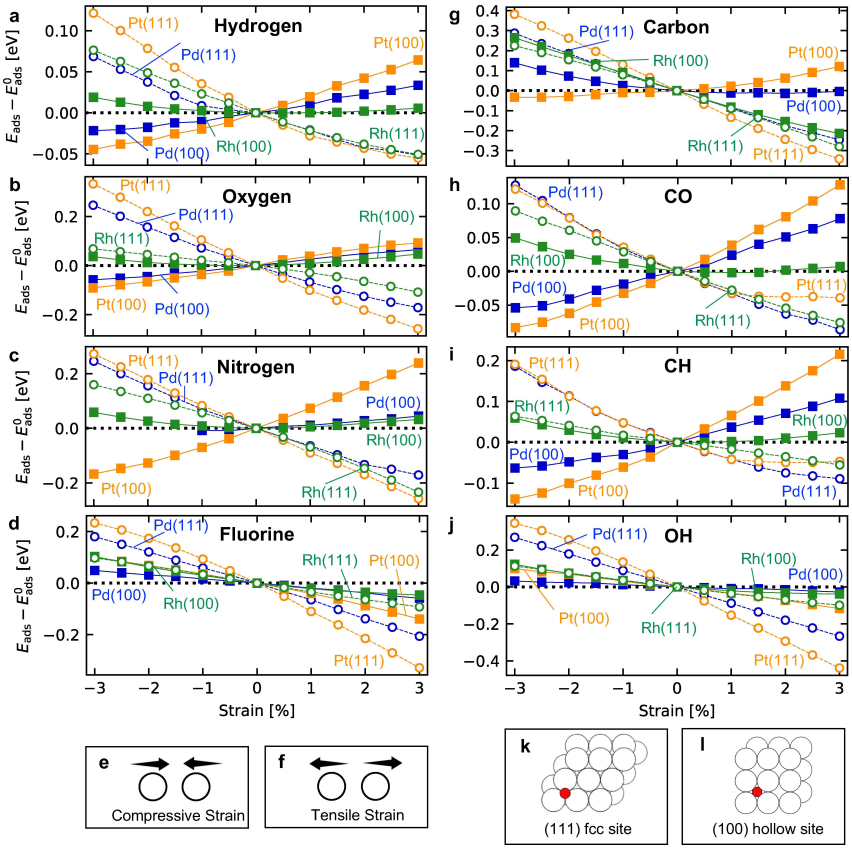

Figure 1. Strain dependent relative change of the adsorption energy with respect to the unstrained surface for a) Hydrogen, b) Oxygen, c) Nitrogen, d) Fluorine, g) Carbon, h) CO, i) CH and j) OH. Different metals are indicated with colors: Rh (green), Pd (blue) and Pt (orange) and different surfaces with filled squares for (100) and empty circles for (111) surfaces, respectively. The adsorption is computed at 1/4 coverage for all cases except for N/Pd(100) and O/Pt (100) where instead the coverage is 1/9. e) and f) show schematic illustrations of compressive (negative values) and tensile strain (positive values). k) Schematic of the three-fold hollow fcc site on (111) and l) of the four-fold hollow adsorption site on (100).

Pd(100) and Pt(100), the trend of adsorption energies is *reversed* with respect to the (111) surfaces. Compressive strain leads to stronger bonding, whereas tensile strain reduces the bond strength. The maximal variation in adsorption energy on the (100) surfaces is about half of the (111)-result. The dependence on strain is more complex for H adsorption on Rh(100) as it has a slight minimum.

Oxygen adsorption on the three (100) surfaces shows similar trends as the hydrogen adsorption. To avoid too large surface distortions, adsorption on Pt(100) was in this case calculated with a 1/9 coverage. Considering nitrogen adsorption, Rh(100) shows the similar weak dependence as for hydrogen and oxygen with a slight minimum. The strain dependence for nitrogen on Pd(100) is similar to that on Rh(100). However, the adsorption site is in this case unstable with respect to distortions when the compressive strain is larger than 1%, even for the lower coverage of 1/9. The effect of strain is pronounced for N adsorption on Pt(100) where the energy changes just as much as for the Pt(111) surface, however with reversed sign. In the case of fluorine, the (100) surfaces show the same sign of the strain-dependence as the (111) surfaces, however, with a weaker change in adsorption energy. Carbon shows the largest changes in adsorption energy as a function of strain. Adsorption on Rh(100) has the same dependence as the Rh(111) surface. The dependence on Pd(100) and Pt(100) is weak, having slight minima for tensile (Pd) and compressive (Pt) strain. The results for boron are similar to carbon and given in the SI.

We study two molecular fragments that are related to carbon, namely CO and CH. Both species show a minimum in the strain dependence for Rh(100). The situation is different for Pd(100) and Pt(100) where the adsorbates are stabilized (destabilized) for compressive (tensile) strain. OH adsorption shows weaker but similar trends for the (100) surfaces as for the (111) surfaces.

Our DFT calculations reveal that the effect of strain for the different adsorbates on the (100) surfaces has a larger variation than for the (111) surfaces. In particular, the response to strain could on the (100) surface either strengthen or weaken the adsorbate bond. The similar trend for all (111) surfaces is connected to the smaller site area with respect to the size of the adsorbate. For cases on the (100) surface where the adsorbates are large (OH and F), the same trend as for the (111) surface is observed. It should be noted that the hollow site on (100) is not necessarily the most stable site of the investigated adsorbates. For the investigated atomic adsorbates, B, C, O, and N prefer the hollow positions on Rh(100) and Pd(100). On Pt

© 2020 The Authors. Published by Wiley-VCH GmbH

(100), the hollow position is preferred for B and C. The molecular species CH and OH are preferably adsorbed in the hollow site for all three investigated (100) surfaces. The stable sites within the used computational method for all considered adsorbates are reported in the SI, Tables S1 and S2.

The obtained strain dependences are affected by the considered coverage. Figure S3 compares the dependence for 0.25 and 1 coverage of CH on Pt(100) and shows that the trend could be reversed going to the high coverage limit. As a high coverage reduces the possibility of local distortions, this underlines the importance of structural relaxations as one part of the mechanism for the observed effects.

As already mentioned, trends in the adsorption of atoms and molecules on transition metal surfaces are commonly described with the *d*-band model.[12] It is based on the assumptions that the hybridization between the metal *s*-bands with the adsorbate is similar for all transition metals and that differences can be described using the hybridization with the *d*-band only. The hybridization depends mainly on the relative position of the *d*-band with respect to the Fermi energy, the *d*-band center ε_d. The *d*-band center captures both, the relative position of the adsorbate and metal states and the strength of the coupling matrix element.[28] Applying strain to metal surfaces affects the overlap of the metal orbitals, leading to a change in the *d*-band width and thereby a shift of the *d*-band. An upward shift of the *d*-band center leads in this model to a strengthening of the metal-adsorbate bond.[29] Figure 2a shows the adsorption energy of H with respect to the unstrained case as a function of the *d*-band center. For the (111) surfaces of Rh, Pd and Pt, a positive shift of ε_d leads to increased bond strength. The situation is reversed for the (100) surfaces. For the adsorption on the Pd(100) and Pt(100) surfaces, an increase of ε_d, leads to a decrease in bonding strength. For H on Ru(100), the dependence on the *d*-band center is weak with a slight minimum. Our results show that the adsorption energy may scale either positively or negatively with the *d*-band center.

In this analysis we used all components of the *d*-band. It has been suggested[30] that only *d*-components taking part in the metal-adsorbate bond should be used in the *d*-band center analysis. Figure S6 reports the strain dependence of each component of the *d*-band. All components show similar trends, which means that the reversed trend does not depend on the used component.

To elucidate the observed trends and put them in relation to changes in the coupling matrix element, we consider a simple analytical two-state model.[31] Figure 2b shows the energy function of the distance between two *s*-functions as for the hydrogen-ion molecule. The energy is determined by the two parameters *p* and *q*, which describe the exponential decay of the orbitals ($\varphi = e^{-q/r}$). Fixing the *q*-parameter to 1, representing one specific adsorbate state, the *p*-parameter is varied, representing ε_d. For a fixed distance, enlarging *p* corresponds to reducing the extend of the radial function which leads to a reduced overlap to the adsorbate state. Instead, reducing *p* at a fixed distance, increases the overlap between the two functions. Changing the distance between the orbitals, different *p*-parameters result in different energy curves as

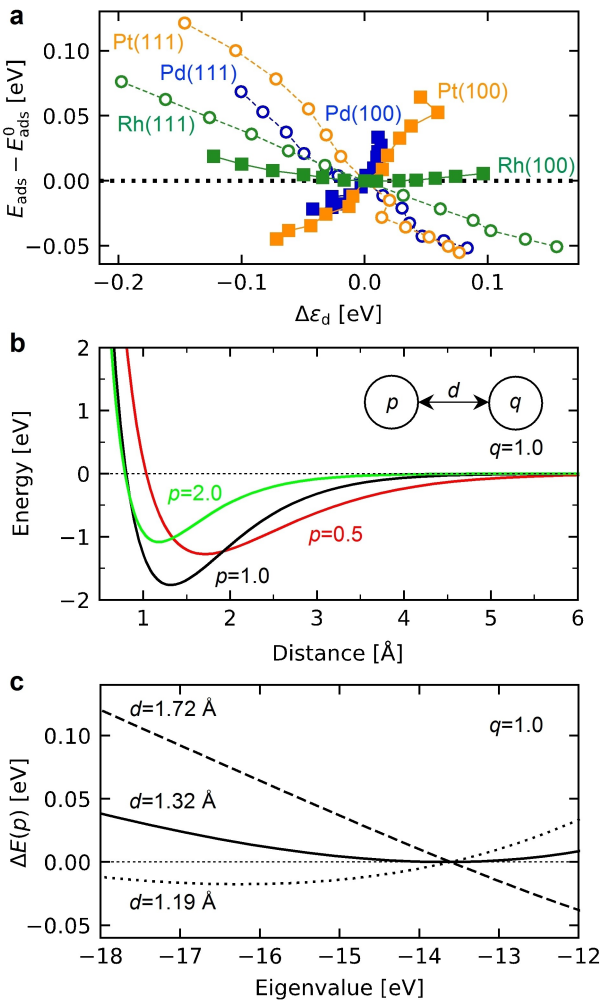

Figure 2. a) Relative change of the Hydrogen adsorption energy with respect to the shift of the d-band center compared to the unstrained surfaces of Rh, Pd and Pt (111) and (100). b) Distance dependant energy between two s-orbitals with characteristic values of q = 1 and p = 0.5,1.0 and 2.0. The minimum corresponding distances are marked as vertical lines. The inset visualizes the used parameters. c) Relative energy to E(−13.6 eV) for fixed distances d = 1.19 Å, 1.32 Å and 1.72 Å, fixed q = 1 and varying p.

shown in Figure 2b. Figure 2c shows the effect on the binding energy when varying the overlap between the two orbitals for three distances. The *p*-parameter is in this case varied, which corresponds to different eigenvalues and consequently different *d*-band centers. The energy is given with respect to the eigenvalue with $p = 1$ (−13.6 eV). Depending on the distance between the orbitals, the relative energies change with different slopes. A distance of 1.32 Å corresponds to the optimal distance between the orbitals, whereas $d = 1.19$ Å is on the repulsive part of the potential energy curve and $d = 1.72$ Å on the attractive part. $d = 1.32$ Å shows a dependence with both negative and positive slopes and a minimum. A similar functional dependence is observed for $d = 1.19$ Å although the dependence is weaker. For $d = 1.72$ Å, the slope is negative over the entire range. This simple two-orbital picture demonstrates that the functional dependence on the eigenvalue of one of the orbitals (*d*-band center) is sensitive to the distance between the

© 2020 The Authors. Published by Wiley-VCH GmbH

orbitals. Different functional dependences arise for different distances, which elucidates the DFT-results for the (100) and (111) surfaces.

Clearly, the applied surface strain changes the overlap between the metal atoms, which changes non-linear with strain.[32] For adsorption on metal surfaces, many atoms contribute to the adsorption energy. The adsorbate is relaxed to a position that minimize the total energy, however, the distances in each two-body interaction are not optimized. This has, in particular, consequences for sites where the adsorbate could interact with subsurface atoms. For an adsorbate in the hollow position of the (100) surface, two opposite effects are contributing to the effect of strain on the bonding. Firstly, with increased tensile strain, the distance of the atoms in the surface increases, which leads to a decreased bond strength. Secondly, counteracting this effect, is the simultaneous reduction of the distance between the adsorbate and the subsurface metal atom, which is strengthened upon tensile strain. Thus, dependent on the size of the adsorbate, the interaction with the subsurface layer may influence the bonding, leading to different functional dependences on strain. Note that the effect of strain for the (100) surfaces follow the (111) surfaces when the adsorbates are electronically large (F and OH). These are cases when the effect of the subsurface atom in the four-fold hollow site on (100) is negligible.

The presented results provide new insights into the understanding of strain effects and site engineering of low-index surfaces, demonstrating that strain has a clear but complex site dependence. We find that different sites may have opposite functional dependences on strain. Given that the active phase in heterogenous catalysts generally are metal nanoparticles with a range of different kinetically coupled sites, these effects should be considered. The observed trends offer new possibilities for catalytic site engineering using strain. Moreover, the results have implications when developing general scaling relations taking strain into account as the strain-response could be structure dependent.

Acknowledgements

Financial support is acknowledged from the Swedish Research Council (2016-5234). The calculations were performed at C3SE (Göteborg) via a SNIC grant. The Competence Centre for Catalysis (KCK) is hosted by Chalmers University of Technology and is financially supported by the Swedish Energy Agency and the member companies AB Volvo, ECAPS AB, Johnson Matthey AB, Preem AB, Scania CV AB and Umicore Denmark ApS.

Conflict of Interest

The authors declare no conflict of interest.

Keywords: computational chemistry · density functional theory · transition metal surfaces · strain · surface science

[1] A. T. Bell, *Science* **2003**, *299*, 1688–1691.
[2] P. L. Hansen, J. B. Wagner, S. Helveg, J. R. Rostrup-Nielsen, B. S. Clausen, H. Topsøe, *Science* **2002**, *295*, 2053 LP–2055.
[3] I. V. Yudanov, M. Metzner, A. Genest, N. Rösch, *J. Phys. Chem. C* **2008**, *112*, 20269–20275.
[4] J. Kleis, J. Greeley, N. A. Romero, V. A. Morozov, H. Falsig, A. H. Larsen, J. Lu, J. J. Mortensen, M. Dułak, K. S. Thygesen, J. K. Nørskov, K. W. Jacobsen, *Catal. Lett.* **2011**, *141*, 1067–1071.
[5] A. Roldán, F. Viñes, F. Illas, J. M. Ricart, K. M. Neyman, *Theor. Chem. Acc.* **2008**, *120*, 565–573.
[6] F. Baletto, R. Ferrando, *Rev. Mod. Phys.* **2005**, *77*, 371–423.
[7] E. M. Dietze, P. N. Plessow, F. Studt, *J. Phys. Chem. C* **2019**, *123*, 25464–25469.
[8] T. Nilsson Pingel, M. Jørgensen, A. B. Yankovich, H. Grönbeck, E. Olsson, *Nat. Commun.* **2018**, *9*, 2722.
[9] I. G. Shuttleworth, *Surf. Sci.* **2017**, *661*, 49–59.
[10] J. R. Kitchin, J. K. Nørskov, M. A. Barteau, J. G. Chen, *Phys. Rev. Lett.* **2004**, *93*, 156801.
[11] M. Mavrikakis, B. Hammer, J. K. Nørskov, *Phys. Rev. Lett.* **1998**, *81*, 2819–2822.
[12] B. Hammer, J. K. Nørskov, *Nature* **1995**, *376*, 238–240.
[13] F. Calle-Vallejo, J. I. Martínez, J. M. García-Lastra, P. Sautet, D. Loffreda, *Angew. Chem. Int. Ed.* **2014**, *53*, 8316–8319; *Angew. Chem.* **2014**, *126*, 8456–8459.
[14] F. Calle-Vallejo, J. Tymoczko, V. Colic, Q. H. Vu, M. D. Pohl, K. Morgenstern, D. Loffreda, P. Sautet, W. Schuhmann, A. S. Bandarenka, *Science* **2015**, *350*, 185 LP–189.
[15] S. G. Wang, B. Temel, J. A. Shen, G. Jones, L. C. Grabow, F. Studt, T. Bligaard, F. Abild-Pedersen, C. H. Christensen, J. K. Nørskov, *Catal. Lett.* **2011**, *141*, 370–373.
[16] S. Schnur, A. Groß, *Phys. Rev. B* **2010**, *81*, 33402.
[17] A. Schlapka, M. Lischka, A. Groß, U. Käsberger, P. Jakob, *Phys. Rev. Lett.* **2003**, *91*, 16101.
[18] F. Calle-Vallejo, A. S. Bandarenka, *ChemSusChem* **2018**, *11*, 1824–1828.
[19] M. Jørgensen, H. Grönbeck, *Angew. Chem. Int. Ed.* **2018**, *57*, 5086–5089; *Angew. Chem.* **2018**, *130*, 5180–5183.
[20] J. P. Perdew, K. Burke, M. Ernzerhof, *Phys. Rev. Lett.* **1997**, *78*, 1396.
[21] G. Kresse, D. Joubert, *Phys. Rev. B* **1999**, *59*, 1758–1775.
[22] G. Kresse, J. Furthmüller, *Comput. Mater. Sci.* **1996**, *6*, 15–50.
[23] G. Kresse, J. Furthmüller, *Phys. Rev. B* **1996**, *54*, 11169–11186.
[24] A. Trinchero, A. Hellman, H. Grönbeck, *Surf. Sci.* **2013**, *616*, 206–213.
[25] M. Monai, T. Montini, R. J. Gorte, P. Fornasiero, *Eur. J. Inorg. Chem.* **2018**, *2018*, 2884–2893.
[26] A. A. Peterson, F. Abild-Pedersen, F. Studt, J. Rossmeisl, J. K. Nørskov, *Energy Environ. Sci.* **2010**, *3*, 1311–1315.
[27] M. Jørgensen, H. Grönbeck, *Top. Catal.* **2019**, *62*, 660–668.
[28] B. Hammer, J. K. Nørskov, *Surf. Sci.* **1995**, *343*, 211–220.
[29] A. Ruban, B. Hammer, P. Stoltze, H. L. Skriver, J. K. Nørskov, *J. Mol. Catal. A* **1997**, *115*, 421–429.
[30] S. E. Mason, I. Grinberg, A. M. Rappe, *J. Phys. Chem. C* **2008**, *112*, 1963–1966.
[31] B. H. Bransden, C. J. Joachain, *Physics of Atoms and Molecules*, Prentice Hall Pearson, London, **2003**.
[32] O. Andersen, O. Jepsen, D. Glötzel, Soc. Italiana Di Fisica, Bologna, Italy, **1983**, p. 59–176.

Manuscript received: August 11, 2020
Revised manuscript received: September 21, 2020
Accepted manuscript online: September 23, 2020
Version of record online: October 7, 2020

© 2020 The Authors. Published by Wiley-VCH GmbH